Kovove Mater. 50 2012 145–152
DOI: 10.4149/km_2012_3_145

Raman spectroscopy used to inspect relationship between surface and magnetic properties of Fe-Nb-Cu-B-Si(4.5) nanocrystalline ribbons

B. Butvinová[1]*, P. Butvin[1], M. Kadlečíková[2], Ľ. Malinovský[1]

[1] *Institute of Physics SAS Bratislava, Dúbravská cesta 9, 845 11 Bratislava, Slovak Republic*
[2] *Institute of Electronics and Photonics FEI, Slovak University of Technology, Ilkovičova 3, 812 19 Bratislava, Slovak Republic*

Received 12 July 2011, received in revised form 14 September 2011, accepted 29 September 2011

Abstract

Many nanocrystalline Fe-Nb-Cu-B-Si ribbons are known to show magnetic anisotropy influenced by macroscopic magnetoelastic interaction. This interaction comes from surfaces exerting force on ribbon interior. Raman spectroscopy is used to investigate surface properties of the 4.5 at.% Si member of Fe-Nb-Cu-B-Si series to indicate sources of the force or the preferred surface crystallization. Hematite and magnetite have been identified on certain surface locations, whereas no Raman response was observed on major surface area. Unlike as-cast state and vacuum annealing, the ferrous oxides appear most abundant after higher temperature Ar annealing similarly as off-axis magnetic anisotropy evolves with annealing. Existence of a silicon oxide layer on the genuine surfaces was excluded by response to intentional deposition of SiO_2. Minor carbon contamination appears to enable ferrous oxides to be revealed by Raman spectroscopy.

K e y w o r d s: nanocrystalline materials, magnetic properties, surface properties, Raman spectroscopy

1. Introduction

Modern Fe-based magnetic materials prepared by the rapid quenching from the melt (RQM) in form of a thin ribbon are already used in industrial production of inductive elements (transformers, chokes, etc.). Very good soft-magnetic properties are obtained when the disordered structure of certain RQM ribbons is transformed to partially nanocrystalline state by appropriate thermal treatment [1]. This necessary technological operation applied to large surface-to-volume ribbon made of chemically reactive material can significantly affect the material homogeneity as, unlike ribbon interior, the surfaces are directly exposed to annealing ambience. Already the precursor on-air prepared RQM ribbon shows surfaces with so-called "native oxide layer" [2] – mostly Fe- and Si-oxides. Whereas non-uniform magnetic anisotropy of an untreated RQM ribbon effectively prevents the effect of surfaces-interior diversity on magnetic properties to be disclosed, thermally treated ribbons show often significantly different magnetic properties due to different annealing ambience. The properties difference is easily emulated by applying a squeezing or spreading resin jacket on the ribbon [3, 4]. The obvious explanation is – there is a mutual force action between the surfaces and interior in many nanocrystallized ribbons. Therefore it is very important to find out in enough detail, what happens to the surfaces during thermal treatment and subsequent cool down. Surface morphology has been the subject of numerous papers [5, 6] and the most frequent observation is – the wheel surface (adjacent to the chill wheel at the RQM process) differs from the air surface (free one exposed to air). Nevertheless, no morphology study points either to correlation to ribbon chemical composition or to systemic changes due to thermal treatment. Unlike the morphology, surface chemistry is shown to change

*Corresponding author: tel.: 02 5941 0560; fax: 02 5477 6085; e-mail address: butvinova@savba.sk

with basic chemical composition as well as with various thermal treatments [7]. Surface chemistry differences and changes thus appear to be more closely associated with the supposed surface-interior force interaction. Apart from the force, a direct impact on magnetic properties can sometimes take place – magnetically harder surfaces form on soft-magnetic interior [8]. External influences can affect the material apart from the thermal treatment. Corrosion studies point preferentially to surface chemistry, too. Si-rich ribbons resist the corrosion better than lower-Si alloys, apparently due to a SiO_2 layer on the ribbon surfaces [9].

This work is devoted to looking for associations between surface chemistry differences and analogously obtained magnetic anisotropy differences on a rarely studied member of the well known alloy series Fe-Nb-Cu-B-Si (Finemet). Due also to published data scarcity we have chosen the Raman spectroscopy to add to the knowledge about Finemet surface chemistry. We tried to recognize what surface-chemistry features can be considered as sources or at least as markers of the associated characteristic magnetic anisotropy.

2. Experimental

Amorphous ribbons of Finemet-type composition $Fe_{78}Nb_3Cu_1B_{13.5}Si_{4.5}$ have been prepared by planar-flow casting on air. Strips of 10 mm width, length is 10 cm and 26.5 μm thickness (it was determined from mass, width, length and density is 7.49 and 7.52 g cm^{-3} for as-cast and annealed ribbon, respectively) were annealed in vacuum or in Ar ambience at 500 ℃ and 540 ℃ for 1 h. Density measurements were made by buoyancy method (Archimedean principle). Hysteresis loops were recorded using a digitizing hysteresis graph at standard ac (21 Hz) sinusoidal H excitation in Helmholtz drive coils along the ribbon long axis. The pick-up coil is coaxial. Investigation of surface chemistry of the strips was performed by Raman spectroscopy using ISA Dilor-Jobin Yvon-Spex Labram confocal system with 15 mW radiation power from He-Ne laser with the back-scattering geometry. Monochromatic 632.8 nm laser beam was focused into a spot with ∼10 μm diameter. Microscope objectives with 10× to 80× magnification were used to observe the beam impact surrounding as well as other characteristic locations on both the strip surfaces – air surface (AS) and wheel surface (WS). Calibration measurements were made by the base wafer of single-crystalline Si (100) with the accuracy ± 2 cm^{-1} and Fe foil (4 μm thickness) to gain reference spectral lines, which are detectable on a similarly conditioned material. All measurements were performed at room temperature.

Acronyms of experimental methods: RS – Raman spectroscopy, CEMS – conversion-electron Mössbauer spectroscopy, XPS – X-ray photoelectron spectroscopy, XRD – X-ray diffraction.

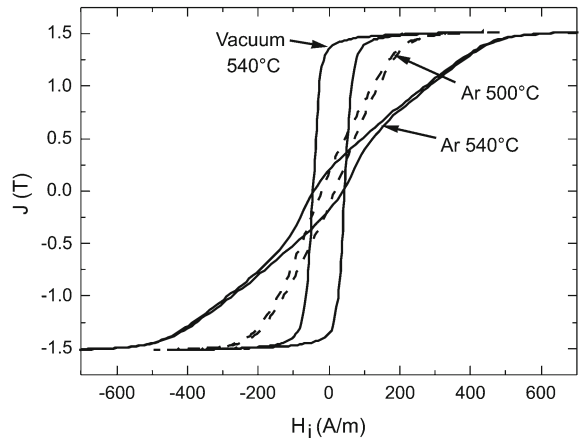

Fig. 1. Hysteresis loops (21 Hz) of strip samples annealed at the indicated temperature and ambience for 1 h.

3. Results and discussion

3.1. Magnetic anisotropy

Nanocrystalline $Fe_{78}Nb_3Cu_1B_{13.5}Si_{4.5}$ ribbon annealed in the different atmosphere manifest either upright (in vacuum) hysteresis loop or slant (in Ar) one – Fig. 1. Different annealing ambience results in different magnetic anisotropy as a rule. Magnetization work W evaluated from saturated loop is used to quantify the density of the off-axis anisotropy energy, which causes the loop tilt. Whereas vacuum annealing brings about negligible loop tilt only (W = 14 J m^{-3}), Ar annealing results in significant anisotropy after 500 ℃ (W = 145 J m^{-3}) and still more after 540 ℃ annealing: W = 310 J m^{-3}. Such off-axis anisotropy comes most often by magnetoelastic interaction $\lambda \times \sigma$ engaged by surfaces and adjacent layers if they squeeze (in-plane compression σ) the deeper interior of a positively magnetostrictive ribbon, which is our case (coefficient of saturation magnetostriction $\lambda_s \sim 10^{-5}$ [3]). Thus there must be a difference between surfaces and interior for the anticipated mutual force to be supported. Indeed, the material studied has been found tending to preferred surface crystallization (of bcc Fe) by CEMS particularly at non-vacuum annealing [10]. The reason for this preference as well as whether this is the sole source of the mutual force is still unclear. Anyway, surfaces often differ from ribbon interior, thus we speak about macroscopic heterogeneity (MH). Although Fe oxides and oxyhydroxides are suspect to persist on ribbon surfaces [2, 7], these substances have not been clearly identified by CEMS or XRD after standard anneal-

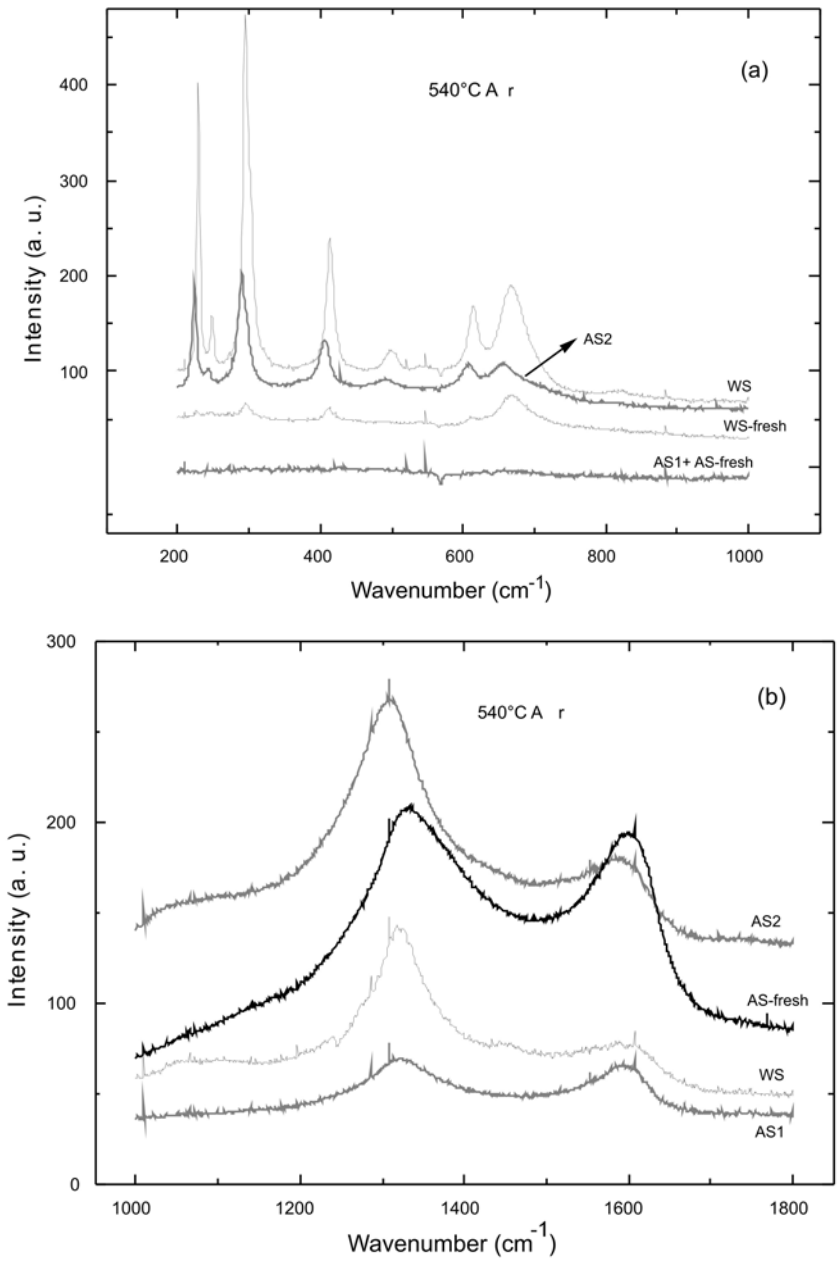

Fig. 2. Raman spectra of the sample annealed at 540 °C for 1 h in Ar. Measurement range: 200–1000 cm^{-1} (a) and 1000–1800 cm^{-1} (b). Labels AS, WS are explained in part 2, AS – fresh in part 3.2.1. The intensity scale is uniform but some curves were shifted to be discernible.

ing so far. Since corrosion experiments [9, 11] have shown significant response, we tested a pair of samples whether their loops changed after prolonged exposure to normal humid ambience. If compared to Fig. 1, no clear, the less one-way changes of the loop tilt have been observed.

3.2. Spectroscopic surface characterization

Earlier spectroscopic investigations revealed certain characteristic substances on Finemet ribbon surfaces. Hematite (α-Fe_2O_3) or maghemite (γ-Fe_2O_3) are the most frequently indicated Fe-oxides by XPS [2, 7] on as-cast and sub-crystallization annealed (≤ 400 °C) ribbons. Other ferrous oxides or FeOOH oxyhydroxides are observed in corrosion experiments on Finemets or alike alloys by XPS, RS and CEMS, too – magnetite (Fe_3O_4) and lepidocrocite [9, 11, 12]. Another oxyhydroxide – goethite is expected in Finemets and can readily be resolved by RS from lepidocrocite [13], but it is hardly discernible from Fe_2O_3 [14] and was not confirmed by other spectroscopic methods [11]. On Si-rich (> 13 at.%) compositions, the formation of a SiO_2 layer is assumed or concluded

[9, 11], but details as to the layer continuity or surface coverage remain unclear. Last but not least carbon should be mentioned. Although no C is added to the basic Fe-Nb-Cu-B-Si composition, it is revealed by XPS despite of ion-bombardment surface cleaning [7]. Graphitic carbon (GC) can be indicated by a characteristic (~ 1300 and $\sim 1600\,\mathrm{cm}^{-1}$) RS twin peak [16] and possible GC occurrence is not commented in RS investigations of Finemet ribbons so far (e.g. [12]).

3.2.1. Raman spectroscopy results – ferrous compounds

No discernible Raman spectrum has been observed on many inspected surface locations – the response shows nothing apart from some photoluminescence (Fig. 2 AS1). Such locations correspond mostly but not exclusively to the majority ribbon-surface area lacking eye-catching features as shown on images of Fig. 3. Apart from shadows due to pronounced surface profile, distinctive features of an optical micrograph appear as dark spots ranging from solitary occurrence (Fig. 3a) to worm-pack-like pattern (Fig. 3c). If locations within these features are inspected by RS, distinctive spectrum is revealed in most cases. Standard macroscopically heterogeneous nanocrystalline sample shows the spectra displayed in Fig. 2. Hematite (α-Fe_2O_3) and magnetite (Fe_3O_4 blend) spectra fit best the peaks of curves for WS and AS2 locations if known data (Table 1 and e.g. [13, 14]) are consulted. Both these locations are found within the dark spots unlike AS1 location, which represents the majority surface area. Magnetite often comes together with Fe_2O_3, which is the standard product of further oxidized magnetite [9]. There is some doubt as to the origin of magnetite in Finemet ribbons since XPS studies do [7] and do not [2] report Fe^{2+} necessary for the magnetite to be indicated. Magnetite can be formed from goethite when appropriately heated [14]. As the goethite belongs to humid ambience products, the question arose, whether long-term exposure to normal laboratory ambience (we do not use desiccator) can bring oxyhydroxides. Thus reference measurement immediately after the standard annealing was performed – labelled "fresh" in Fig. 2. Sole magnetite has been observed on wheel side only. 500 °C Ar annealing was inspected, too (spectra not shown, see Table 1 for band positions). Apart from some weakly pronounced peaks observed on air side, the sample is characterized by clearly identified magnetite again on wheel side only. The generally lower peaks intensity and the absence of detectable Fe oxides on air side point to a less advanced formation of surface products capable of providing sufficient Raman response. Therefore we adhere to the opinion that magnetite is intrinsic [7] and is not preferentially formed from other Fe compounds present on the surface. The result of standard (540 °C) vacuum annealing is displayed in Fig. 4. The well-resolved spectrum was obtained inspecting solitary dark spots (Fig. 3a) on ribbon's wheel side – WS2. The spectrum most probably belongs mainly to hematite. Two features – relative intensity and large width of the peaks just below 400 and $600\,\mathrm{cm}^{-1}$ – do not fit hematite spectrum

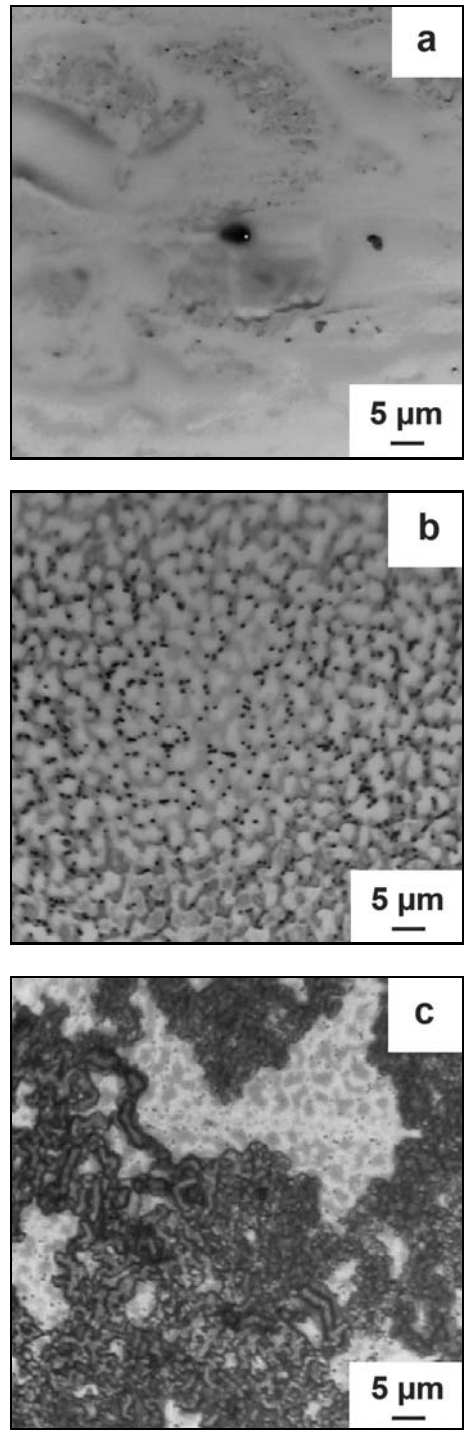

Fig. 3. Images of the surfaces of samples annealed at 540 °C: in vacuum WS (a), fresh Ar annealing AS (b), aged Ar annealing AS (c).

Table 1. Positions of bands in the Raman spectra of $Fe_{78}Nb_3Cu_1B_{13.5}Si_{4.5}$ alloy

vac_540		Ar_540		Ar_540 fresh		Ar_500		Fe foil	[14, 15] (λ_0 = 632.8 nm)
AS	WS2	AS2	WS	AS	WS	AS	WS	Corros.	Fe_2O_3
–	219	222	229	–	225w	–	–	225	227
–	–	242	248	–	245w	266w	–	–	246
–	283	290	295	–	295	315w	–	290	293
–	390	406	413	440m	412	–	–	406	412
–	485w	490w	500	–	–	–	–	494	498
–	593m	607	614	–	–	–	–	606	610
–	–	655	668	–	668	755w	668	656	–
–	1300	1314	1319	1332	1323	1337	1345	1304	1322
–	1597w	1594	1597	1597	1597	1594	1595	–	–

Commentary: w – weak, m – medium

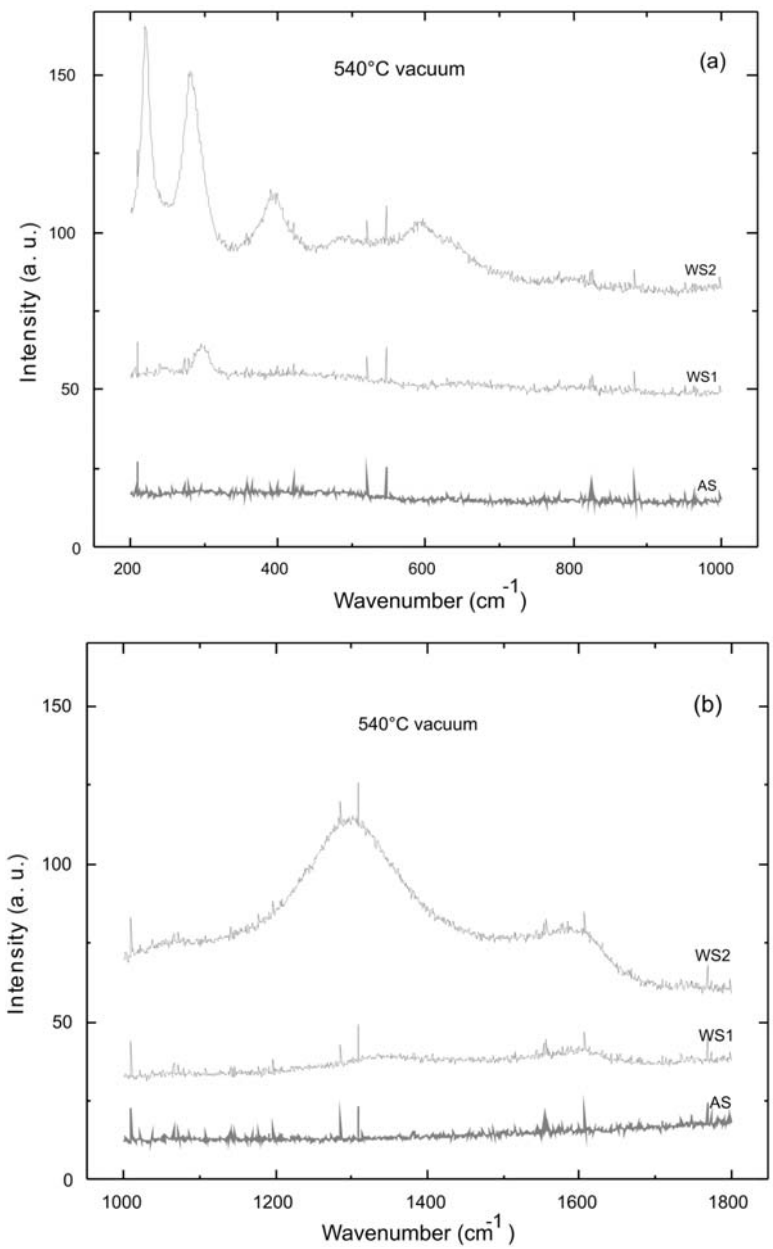

Fig. 4a,b. Raman spectra of the sample annealed at 540°C for 1 h in vacuum. Raman spectrum WS2 was collected from the dark spot (Fig. 3a). Measurement ranges as in Fig. 2ab.

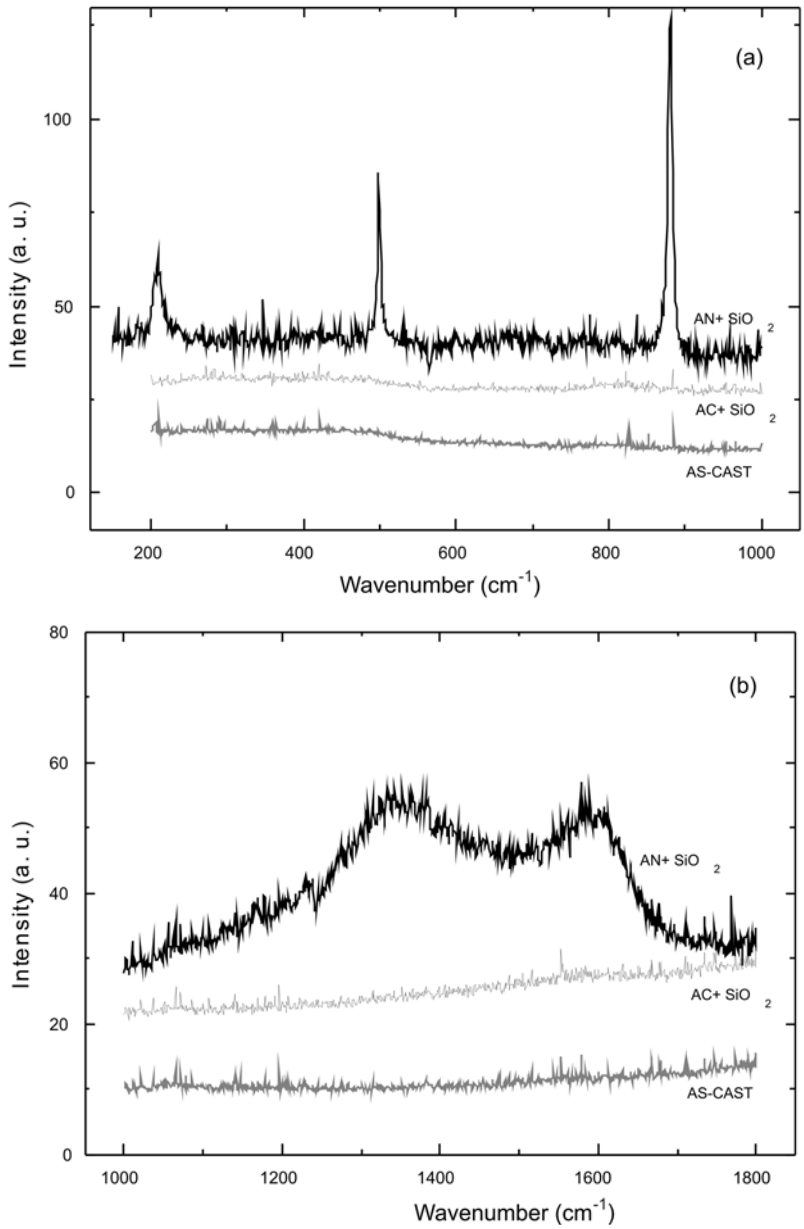

Fig. 5a,b. Raman spectra of the as-cast sample and that one with SiO_2 layer (AC + SiO_2). Sample with SiO_2 layer annealed at 540 °C in Ar for 1 h (AN + SiO_2). Measurement ranges as in Fig. 2ab.

well. Goethite can influence the peaks and chances are that some goethite could be formed during the time between annealing and RS measurement in normal humid ambience. This applies to WS1 location, which shows small peak below 300 cm^{-1}, however, to a lesser extent since goethite's usually major peak at 386 cm^{-1} [13] is lacking at WS1 completely. Perfect complete Raman spectra could hardly be expected on standard Finemet surfaces, the less on the vacuum-annealed sample where its surface is still up to 70 % amorphous, too [10]. Many distinctive Raman modes are simply not supported by such a structure. The air side looks just like this – obviously no Raman modes are supported.

3.2.2. Raman spectroscopy results – graphitic carbon

As seen in Fig. 2b as well as in Fig. 4b, the 1300–1600 cm^{-1} twin peak is observed more generally than the Fe-oxides peaks. Nevertheless, the twin peak is higher and its 1300 cm^{-1} part is better pronounced when Fe oxides are indicated, too. Whereas Fe_2O_3 and goethite can add to the lower-wavenumber peak (Table 1), the twin peak itself is most straightforwardly explained by GC. The 1600 cm^{-1} G band is assigned to polycrystalline graphite, the other peak (D band) to a disordered, defect-rich graphite [16]. There are several possibilities for carbon to come into contact and adhere to the ribbon surface. We prefer

to leave the ribbon surface as is and do not apply methods unusual at standard fabrication of magnetic cores. Although contamination (e.g. by fingerprints) is avoided, no devoted surface cleaning is performed before annealing. Thus contamination by air pollutants contained for instance in atmospheric aerosols [16] is not prevented. The non-evacuated annealing furnace can collect some remnants of burned carbonaceous pollutants despite of standard cleaning. Certain other results gained in this work point to an external GC source: there is no twin peak on as-cast samples (Fig. 5), apart from a solitary spot, no GC is indicated after vacuum annealing (Fig. 4) and the reference Fe foil shows (Table 1) only the 1300 cm^{-1} peak attributable to Fe_2O_3 or to disordered GC as well. The foil has not been annealed and so no better-ordered GC can show its 1600 cm^{-1} peak. We thus assume that GC comes by surface contamination and, contrary to [7], we found no reason to consider it intrinsic. XPS investigations gained good arguments in favour of Fe oxides present already in the as-cast state [2, 7] though RS has identified no Fe oxides on virgin as-cast ribbons so far. In the same spirit, we have not observed any Fe-oxide Raman spectra not to be accompanied by the GC twin peak on nanocrystallized samples investigated so far. Thus it appears that the GC-affected surface locations are advantageous for the Fe oxides to become more easily ordered so as to show up in RS. This by no means excludes the presence of Fe oxides and/or oxyhydroxides on locations where no RS indication was gained. What is the significance of the assumed RS-detectable Fe oxide – GC "cooperation" for the macroscopic force, which is exerted by surfaces on ribbon interior, remains an open question worth of further research including the cooperation mechanism, too.

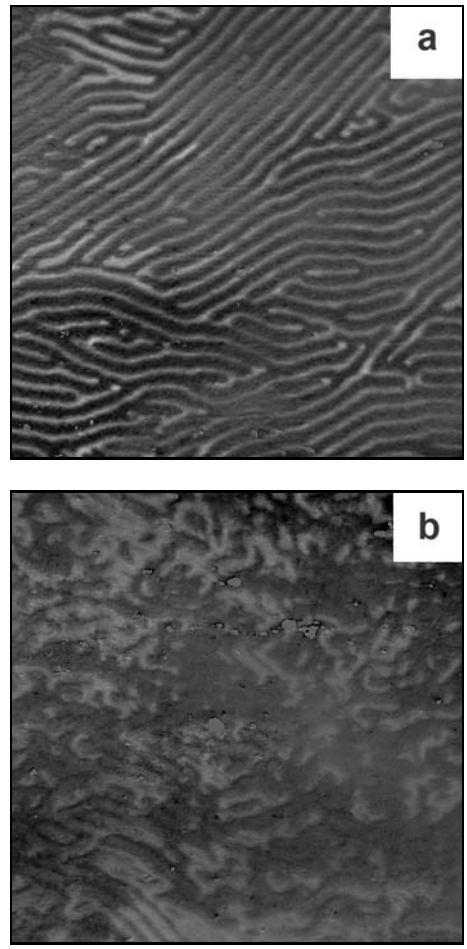

Fig. 6. Domain structure on the air side of sample annealed at 540 °C for 1 h in Ar, which was observed by RS (see Fig. 2). (a) and (b) refer to separate places 4 mm apart. Recorded by digitally enhanced MOKE method [17]. Actual size of area displayed: 0.5 × 0.5 mm^2.

3.2.3. Raman spectroscopy results – silicon oxide

To see what could be the effect of a compact silicon oxide layer [9] on Raman observation, SiO_2 was vapour deposited on a pair of as-cast samples. No discernible Raman peaks were observed soon after the deposition although many locations were inspected. Standard 540 °C Ar annealing made the GC twin peak to appear clearly and without any characteristic Fe oxides spectra from a selected suspect (dark) location. Instead, three narrow, unidentified yet peaks (at 210, 500 and 880 cm^{-1}) appeared there at lower wavenumbers but at reduced incident laser power (4 mW) only – Fig. 5. The three narrow peaks were observed on "normal" bright locations, too, however, without the GC twin peak. The explanation offered: the graphitic carbon is an external contamination, it neither contributes the Fe oxides nor it promotes ribbon-intrinsic Fe oxides ordering when separated from them. The artificial silicate structure is continuous but "thermally shy" and it is not ordered and firm enough to support characteristic Raman vibrational modes after the annealing targeted solely to nanocrystallize the metallic ribbon substrate. Comparison of the above results to surface-untreated ribbons leads us to the conclusion that there is no significant surface Si oxide formation on the studied low-Si (4.5 at.%) ribbons during any of the annealing procedures performed in this work.

3.3. Surface chemistry and magnetic properties

Raman spectroscopy thus endorses the earlier XPS results on amorphous samples – Fe oxides and possibly oxyhydroxides too are present on the very surfaces of a Finemet ribbon also when partly nanocrystallized. This finding does not provide a decisive answer to the question whether the surface-oxide formation at annealing relies on intrinsic or ambient oxygen to explain

the systemic difference in MH between vacuum- and Ar-annealed ribbons. Although an essential contribution of the RS-confirmed Fe oxides to the macroscopic force that causes the characteristic anisotropy is less probable due to minor only occurrence on surfaces, a direct influence is possible. Magnetic Fe oxides of any structure are significantly magnetically harder than the basic Fe-Nb-Cu-B-Si material. Unlike magnetite, disordered hematite does not show magnetic domain structure due to its low magnetic moment. Figure 6a shows typical surface closure domains where external field necessary to move and finally erase the structure was an order higher than the field that saturated the sample major volume – the surface is magnetically harder. Magnetically still harder surface is observed on other places of the same sample. Moreover, the domain walls pronounced by so-called V-lines [17] in the left half of Fig. 6b become hardly discernible in the right half. The probable reason is the building of a surface layer, which does not support well visible domain structure. Such a behaviour can readily be anticipated for a layer of disordered hematite (observed on this ribbon near its edges). To explain the difference between air and wheel surfaces has not been the scope of this work. Still we assume that the more frequent appearance of RS-detectable Fe oxides on the wheel side is due to air pockets confined between wheel and ribbon at its fabrication and the far more edged profile of this side.

4. Conclusions

– Compounds with structures supporting Raman vibrational modes are rare on standard surfaces of as-cast or nanocrystallized Finemet ribbons. Therefore possibilities to observe Raman spectra are limited to certain special surface locations or a devoted surface treatment is necessary.

– The observed Raman spectra endorse earlier XPS findings and identify hematite and magnetite to be present on surfaces of nanocrystalline ribbons without dedicated exposure to a corrosive ambience. The surface oxides are capable of influencing the magnetic properties although indications were only gained.

– Minor surface contamination by graphitic carbon has proven advantageous for obtaining usable Raman spectra from otherwise unresponsive Finemet surfaces. The effect necessitates and deserves further research.

Acknowledgements

The authors are grateful for partial financial support to VEGA grants No 2/0056/11 and 1/0746/09. Magnetic domain structures were observed and evaluated by the courtesy of Dr Rudolf Schäfer in his laboratory in IFW Dresden, Germany.

References

[1] Herzer, G.: Nanocrystalline Soft Magnetic Alloys in Handbook of Magn. Mater., Vol. 10. Amsterdam, Elsevier Science 1997.

[2] Jain, R., Saxena, N. S., Rao, K. V. R., Avasthi, D. K., Asokan, K., Sharma, S. K.: Mat. Sci. Eng., *A297*, 2001, p. 105. http://dx.doi.org/10.1016/S0921-5093(00)01262-4

[3] Butvin, P., Butvinová, B.: J. Electrical Engineering, *50*, 1999, 8/S, p. 119.

[4] Butvin, P., Butvinová, B., Sitek, J., Degmová, J., Vlasák, G., Švec, P., Janičkovič, D.: J. Magn. Magn. Mater, *320*, 2008, p. 1133. http://dx.doi.org/10.1016/j.jmmm.2007.10.026

[5] Pavúk, M., Miglierini, M., Vujtek, M., Mashlan, M., Zboril, R., Jiraskova, Y.: J. Phys. Condens. Mater, *19*, 2007, p. 216219. http://dx.doi.org/10.1088/0953-8984/19/21/216219

[6] Paluga, M., Švec, P., Janičkovič, D., Mrafko, P., Conde, C. F.: J. Non-Crystal. Sol., *353*, 2007, p. 2039. http://dx.doi.org/10.1016/j.jnoncrysol.2007.01.068

[7] Chenakin, S. P., Galstyan, G. G., Tolstogouzov, A. B., Kurse, N.: Surf. Interface Anal., *41*, 2009, p. 231. http://dx.doi.org/10.1002/sia.3012

[8] Životský, O., Postava, K., Kraus, L., Malátek, M., Janičkovič, D., Ciprian, D., Luňáček, J., Pištora, J.: J. Magn. Magn. Mater, *290–291*, 2005, p. 625. http://dx.doi.org/10.1016/j.jmmm.2004.11.316

[9] May, J. E., Nascente, P. A. P., Kuri, S. E.: Corrosion Science, *48*, 2006, p. 1721. http://dx.doi.org/10.1016/j.corsci.2005.05.024

[10] Butvin, P., Butvinová, B., Frait, Z., Sitek, J., Švec, P.: J. Magn. Magn. Mater, *215–216*, 2000, p. 293. http://dx.doi.org/10.1016/S0304-8853(00)00137-2

[11] Sitek, J., Sedláčková, K., Seberíni, M.: Czechoslovak J. Phys., *55*, 2005, p. 883. http://dx.doi.org/10.1007/s10582-005-0090-2

[12] Altube, A., Takenouti, H., Beaunier, L., Keddam, M., Joiret, S., Borensztajn, S., Pillier, F., Pierna, A. R.: Corrosion Science, *45*, 2003, p. 685. http://dx.doi.org/10.1016/S0010-938X(02)00146-4

[13] Wang, A., Haskin, L. A., Jollif, B. L.: Lunar and Planetary Sci., XXIX, 1998, abstract 1819 (http://www.lpi.usra.edu/meetings/LPSC98/pdf/1819.pdf).

[14] De Faria, D. L. A., Lopes, F. N.: Vibrational Spectroscopy, *45*, 2007, p. 117. http://dx.doi.org/10.1016/j.vibspec.2007.07.003

[15] Legodi, M. A., De Waal, D.: Dyes and Pigments, *74*, 2007, p. 161. http://dx.doi.org/10.1016/j.dyepig.2006.01.038

[16] Metres, S., Dippel, B., Schwarzenböck, A.: Aerosol Sci., *35*, 2004, p. 347. http://dx.doi.org/10.1016/j.jaerosci.2003.10.002

[17] Hubert, A., Schäfer, R.: Magnetic Domains. Berlin, Springer-Verlag 1998.